J Fluoresc (2012) 22:431–441
DOI 10.1007/s10895-011-0976-2

ORIGINAL PAPER

Conformational Transitions of the Catalytic Domain of Heme-Regulated Eukaryotic Initiation Factor 2α Kinase, a Key Translational Regulatory Molecule

R. K. Sreejith · C. G. Suresh · Siddharth H. Bhosale · Varsha Bhavnani · Avinash Kumar · Sushama M. Gaikwad · Jayanta K. Pal

Received: 10 June 2011 / Accepted: 13 September 2011 / Published online: 23 September 2011

Abstract In mammalian cells, the heme-regulated inhibitor (HRI) plays a critical role in the regulation of protein synthesis at the initiation step through phosphorylation of α-subunit of the eukaryotic initiation factor 2 (eIF2). In this study we have cloned and performed biophysical characterization of the kinase catalytic domain (KD) of rabbit HRI. The KD described here comprises kinase 1, the kinase insertion domain (KI) and kinase 2. We report here the existence of an active and stable monomer of HRI (KD). The HRI (KD) containing three tryptophan residues was examined for its conformational transitions occurring under various denaturing conditions using steady-state and time-resolved tryptophan fluorescence, circular dichroism (CD) and hydrophobic dye binding. The parameter A and phase diagram analysis revealed multi-state unfolding and existence of three stable intermediates during guanidine hydrochloride (Gdn-HCl) induced unfolding of HRI (KD). The protein treated with 6 M Gdn-HCl showed collisional and static mechanism of acrylamide quenching and the constants (K_{sv}=3.08 $M^{-1}$and K_s= 5.62 M^{-1}) were resolved using time resolved fluorescence titration. Based on pH, guanidine hydrochloride and temperature mediated transitions, HRI (KD) appears to exemplify a rigid molten globule-like intermediate with compact secondary structure, altered tertiary structure and exposed hydrophobic patches at pH 3.0. The results indicate the inherent structural stability of HRI (KD), a member of the class of stress response proteins.

Keywords eIF2α kinase · Heme-regulated inhibitor · Steady-state and time-resolved fluorescence · Circular dichroism (CD) · Molten globule

Introduction

In eukaryotic cells, protein synthesis is shut off when cells experience an emergency due to various cellular stresses [1, 2]. An important contributor to stress adaptation is a family of protein kinases that phosphorylate the eukaryotic initiation factor 2α-subunit (eIF2α).[1] Four eIF2α kinases, GCN2, PERK, PKR and HRI, are known to phosphorylate the Ser51 residue specifically in response to diverse stress conditions such as amino acid starvation, endoplasmic reticulum stress, viral infection and heme deficiency, respectively. Although these four kinases have similar kinase domains, their sensing functions and domains differ [3–7].

Electronic supplementary material The online version of this article (doi:10.1007/s10895-011-0976-2) contains supplementary material, which is available to authorized users.

R. K. Sreejith · V. Bhavnani · J. K. Pal
Department of Biotechnology, University of Pune, Pune, Maharashtra 411007, India

C. G. Suresh · S. H. Bhosale · A. Kumar · S. M. Gaikwad (✉)
Division of Biochemical Sciences, National Chemical Laboratory, Pune, Maharashtra 411008, India
e-mail: sm.gaikwad@ncl.res.in

J. K. Pal (✉)
Molecular Cell Biology Laboratory, Department of Biotechnology, University of Pune, Pune 411007, India
e-mail: jkpal@unipune.ac.in

[1] Abbreviations used: eIF2α, eukaryotic initiation factor 2alpha; GCN2, general control non-derepressible-2; PKR, dsRNA-dependent protein kinase; PERK, PKR-like endoplasmic reticulum kinase; HRI, heme-regulated inhibitor; KD, kinase catalytic domain; Gdn-HCl, guanidine hydrochloride; ANS, 1-anilino 8-naphthalene sulfonic acid.

HRI, the heme-regulated inhibitor of translation, is highly expressed in the erythroid precursors, which causes the inhibition of protein synthesis at the initiation step during iron/heme deficiency [8]. HRI is a Ser/Thr kinase and a dimer of ~90 kDa polypeptide [9]. Although HRI is reported to sense the heme concentration in erythroid precursors [10, 11], it is found in various other tissues, including the brain, lung, heart, liver, spleen, kidney, thymus, stomach, pancreas, colon, testis, and uterus [12–14]. In addition to heme deficiency, HRI is also activated under conditions of a variety of other stresses, such as heavy metal exposure, heat shock and oxidative stress [15–17]. The active full length HRI exists as a non-covalently linked dimer whereas the inactive HRI exists as a disulfide linked dimer [18]. We report here for the first time the presence of an active monomer of HRI (KD). Although various biochemical studies have provided valuable information regarding the regulation and activation of HRI, there are no studies regarding the structural characterization of HRI till date. In the present investigation, we have studied these aspects of HRI (KD) occurring under different denaturing conditions by various biophysical methods. We have already studied the substrate of this kinase (eIF2α) in detail and reported that the protein existed in a molten globule state at pH 2.0 and shows an inherent structural stability [19]. In this study, we began with the observation that the kinase catalytic domain (KD) of HRI can function as an active kinase and is regulated by heme. Therefore KD domain was chosen for further studies. Our results indicated that HRI (KD) existed as a monomer of 55 kDa. The biophysical and biochemical studies presented herein provide an important insight into the structural dynamics of protein in solution; including the formation of stable unfolding/refolding intermediates.

Materials and Methods

Materials

Escherichia coli BL21 Rosetta cells and pET 28a vector were obtained from Novagen, Germany. Primers specific to rabbit HRI (KD), guanidine hydrochloride (Gdn-HCl), 1-anilino 8-naphthalene sulfonic acid (ANS), anti-phosphothreonine and -phosphotyrosine antibodies and all chemicals used in quenching studies were purchased from Sigma Chemical Co. (USA). Phospho-eIF2α (Ser51) antibody was purchased from Cell Signaling Technologies, USA. BM Chemiluminescence Western blotting kit (Mouse/Rabbit) was purchased from Roche Molecular Biochemicals (Germany). Ni-NTA agarose and gel extraction kit were purchased from Qiagen, Germany. HRI cDNA clone and its full sequence have been published earlier [4].

Methods

Cloning, Protein Expression and Purification of HRI (KD)

Rabbit HRI (KD) (1230 bp) was PCR amplified using specific primers 5′-ATTCCATATGGAGTTTGAAGAGCTCTC CATC-3′ and 5′-CCGCTCGAGGAAGAGCTCACTCTGC-3′ (Nde1 and Xho1 sites are underlined) from HRI-cDNA and cloned into the pET 28a expression vector. The clones were confirmed by DNA sequencing and they were transformed into *E. coli* BL21 Rosetta cells for expression. Expression and purification was performed as described elsewhere with slight modifications [20].Briefly, the inclusion body solubilization buffer and Ni-NTA agarose column equilibration buffer contained 6 M guanidine hydrochloride (Gdn-HCl) whereas the wash and elution buffers contained 8 M urea as the denaturant. Nickel bound proteins were removed with wash buffer containing 20 mM imidazole and the pure His-tagged protein was eluted with 400 mM imidazole. The purified proteins were refolded by using a rapid dilution method (1:50) as reported earlier [21]. Essentially, the purified protein was suspended slowly in the refolding buffer (pH 8.0) consisting of 0.02 M ethanolamine, 1 mM EDTA, 0.5 M L-arginine, 5 mM reduced glutathione, and 0.5 mM oxidized glutathione and left static for 36 h at 4 °C. The refolded protein was concentrated, dialyzed against phosphate-buffered saline (PBS), pH 7.4 and subjected to SDS-PAGE, circular dichroism, and mass spectrometric analysis. We used classical size exclusion chromatography (SEC) on Protein Pack SW300 (Waters, USA) to evaluate the oligomeric state of the purified protein. The mobile phase used was 10 mM PBS, pH 7.4 and a 100 μl sample of protein solution (50 μM) was applied to the column.

Protein Kinase Assays and Western Blot Analysis

In order to confirm the functionality of the refolded protein, the autokinase and eIF2α kinase activities of the purified and refolded HRI (KD) were performed as described previously with slight modifications [19]. Along with other components, the kinase assay reaction mixture contained rabbit HRI (KD) (1 μg) and purified human eIF2α (heIF2α) (3 μg). The assay mixture was subjected to 10% SDS-PAGE [22] and the proteins were electrophoretically transferred onto nitrocellulose membranes [23]. Blots were immunoreacted with anti-phosphothreonine, -phosphotyrosine and -phospho eIF2α (Ser51) antibodies, and HRP-conjugated secondary antibody, and developed using the chemiluminescence detection kit. Results were analyzed using Bio-Rad gel documentation system (USA).

Fluorescence Measurements

Fluorescence spectra measurements were performed on a PerkinElmer LS-50B spectrofluorometer equipped with a thermostatically controlled sample holder at 25 °C. The excitation wavelength was 295 nm and the emission spectra were recorded between 300 and 400 nm. Both the excitation and emission spectra were obtained setting the slit-width at 7 nm, and scan speed 100 nm min^{-1}. The protein concentrations in the fluorescence measurements were in the range 0.01–0.03 mg/ml.

The decomposition of Trp fluorescence spectra was carried out using PFAST program (http://pfast.phys.uri.edu/pfast/) developed based on the SIMS and PHREQ spectral decomposition methods as described elsewhere [24].

For ANS fluorescence in the hydrophobic dye binding experiments, the excitation was set at 375 nm and the emission spectra were recorded in the range 430–550 nm. The samples were incubated for 4 h at different pH conditions (50 mM buffers). Since the fluorescence intensity was very high and beyond the limit of calculation, the protein concentration was reduced to 0.005 mg/ml for pH 3.0 incubated samples.

Base line correction was performed using the appropriate reaction mixtures for all the data collected.

Parameter A and Phase Diagram Analysis

Parameter A and phase diagram were used to monitor protein conformational changes and to detect folding intermediates as described elsewhere [25–28]. Parameter A is the ratio of the intensity at 320 nm to that at 365 nm of the intrinsic fluorescence (I_{320}/I_{365}). The phase diagram was constructed by the fluorescence intensity at 320 nm versus that at 365 nm at different Gdn-HCl concentrations. The fluorescence data was normalized by the corresponding intensity of the protein spectrum recorded in the absence of Gdn-HCl.

Quenching Experiments

Fluorescence quenching measurements were performed for native and 6 M Gdn-HCl denatured protein with different quenchers like acrylamide, iodide and cesium. The spectra measurements were performed as described in section of Fluorescence measurements. Fluorescence titration was performed by adding aliquots of 5 M quencher to the protein sample (0.03 mg/ml) prepared in 50 mM phosphate buffer, pH 7.4. Sodium thiosulfate (0.2 M) was added to the iodide stock solution to prevent the formation of tri-iodide (I^{-3}). Relative fluorescence intensities were measured at the wavelength corresponding to the emission maximum (342 nm) of the protein and volume correction for fluorescence intensities was done before analyzing the quenching data.

Lifetime Measurement

Lifetime fluorescence measurements were carried out by employing CW-passively mode-locked frequency-doubled Nd: YAG laser (Vanguard, Spectra Physics, USA)- driven rhodamine 6 G dye laser which generates pulses of width ~1 ps. Fluorescence decay curves were obtained by using a time-correlated single-photon counting set up, coupled to a microchannel plate photomultiplier (model 2809u; Hamamatsu Corp.). The instrument response function (IRF) was obtained at 295 nm using a dilute colloidal suspension of dried non-dairy coffee whitener. The half width of the IRF was ~40 ps. Time per channel was40 ps. The samples were excited at 295 nm and the fluorescence emission was recorded at 342 nm. The slit width of emission monochromator was 7 nm. Protein samples at a concentration of 1.8 μM were used for this experiment. The resultant decay curve was analyzed by a multi-exponential iterative fitting program provided with the instrument.

Circular Dichroism (CD) Measurements

The CD spectrum of the protein was monitored in a Jasco 815-150S (Jasco, Tokyo, Japan) spectropolarimeter connected to a Peltier Type CD/FL Cell circulating water bath (Jasco, Tokyo, Japan). Far and near UV CD measurements were recorded using protein concentrations of 0.1 mg/ml and 1.0 mg/ml, respectively. Each spectrum was the average of three scans. The effects of various denaturing conditions and pH on protein were studied as mentioned previously [19]. The secondary structure calculations were done using CDPro program available online. The results are expressed as mean residue ellipticity (MRE).

Results and Discussion

Cloning, Protein Expression and Purification of HRI (KD)

In order to meet the requirement of a large amount of protein for conducting multiple assays, we expressed the protein in *E. coli* using the pET expression system. HRI (KD) (409 amino acids) was cloned, overexpressed and purified. The protein was 95% pure as judged by SDS-PAGE analysis, and it migrated as a single band of 55 kDa on the gel (Supplementary Fig. 1A). The mass of the protein was confirmed by mass spectrometry. The purified protein was refolded according to the method described by White et al. [21]. This method typically provided a 20–25%

yield. The autokinase and eIF2α kinase activities of the purified and refolded HRI (KD) confirmed the activity of the refolded protein (Supplementary Fig. 1B). This data confirmed proper folding and functionality of the protein upon refolding. The kinase catalytic domain (KD) of HRI could function as an active kinase and is regulated by heme as observed by in vitro kinase assay (Supplementary Fig. 1C). The rabbit HRI (KD) phosphorylates human eIF2α used as the substrate here. The SEC studies and SDS-PAGE with or without the reducing agent, β-mercaptoethanol, indicated that HRI (KD) existed as a monomer (Supplementary Fig. 2). Although the molecular mass of HRI (KD) predicted from the amino acid sequence is 46 kDa, a slight variation was observed on SDS-PAGE. The results from SEC studies indicated that the protein used in the present study were soluble and not aggregated.

Gdn-HCl Induced Unfolding

All the three trp residues present in HRI (residues-236, 387 and 389, NCBI ID: AAA31241.1) are located in the catalytic domain. The fluorescence spectrum of the native protein showed maximum intensity at 342 nm (Fig. 1a) indicating trp in the partially hydrophilic environment. The gradual red shift in the λ_{max} of the fluorescence intensity of the protein in presence of increasing concentration of Gdn-HCl is shown in Fig. 1a (inset) which ultimately shifted to 357 nm in presence of 6 M Gdn-HCl, indicating exposure of trps to completely polar environment due to unfolding of the protein. The drastic decrease in the fluorescence intensity of denatured protein was due to the exposure of the side chains of trps to solvent and quenching of fluorescence thereby. The Gdn-HCl induced unfolding of HRI (KD) monitored on the basis of the intrinsic fluorescence intensities at λ_{em}=320 nm and λ_{em}=365 nm (Fig. 1b) show drastic decrease in fluorescence emission in the presence of 0.25 to 0.5 M Gdn-HCl, which is followed by a steep increase at 0.75 M and slow increase up to 1.5 M Gdn-HCl. Further increase in denaturant concentration causes gradual decrease in fluorescence intensity at 320 nm while it decreases marginally up to 6 M Gdn-HCl at 365 nm. The Gdn-HCl mediated unfolding of HRI (KD) may be interpreted as a complex process involving two intermediate conformations, Int_1 and Int_2, which are populated at around 0.25 and 0.75 M Gdn-HCl, respectively. The alteration in the environment of trps at low concentration of the denaturant could be due to the breaking of weak interactions around. The increase in the fluorescence intensity again at 0.75 M could be due to the change in the microenvironment as shown by a red shift in the λ_{max} to 345 nm during unfolding (inset Fig. 1a).

Decomposition analysis of the tryptophan fluorescence spectra of the native protein by PFAST indicated two classes; 18.6% class S which includes buried tryptophan residue(s) or conformers and 81.4% class II containing structured water molecules near to indole ring of trp residue in the protein (Fig. 1c). The successive increase and decrease in the percentage of class S and class II up to

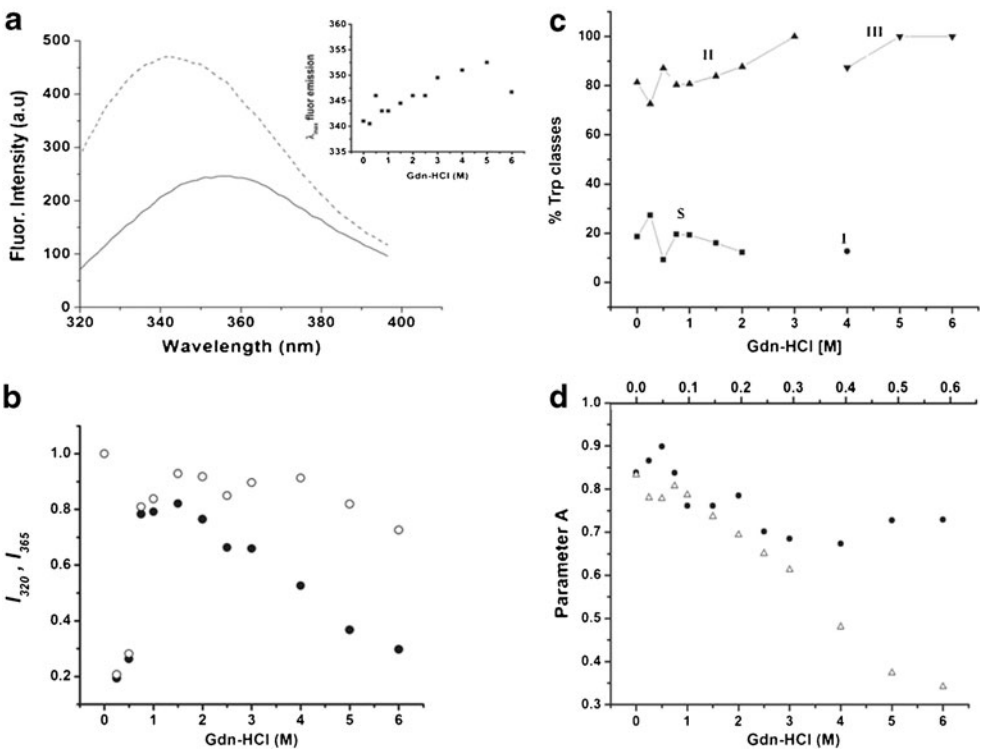

Fig. 1 Effect of Gdn-HCl on equilibrium unfolding of HRI (KD). **a** Fluorescence emission spectra of the native (– – –) and 6 M Gdn-HCl denatured HRI (KD) (——). Inset: λ_{max} shift of intrinsic fluorescence with increasing Gdn-HCl concentration. (B) Change in tryptophan fluorescence at 320 (*filled circles*) and 365 nm (*empty circles*) with increasing concentration of Gdn-HCl. **c** Decomposition analysis showing different classes of the tryptophan fluorescence spectra under varying concentrations of Gdn-HCl. **d** Gdn-HCl induced changes in intrinsic fluorescence parameter A (*empty triangles* and *filled circles* represent unfolding and refolding, respectively). All Protein (0.03 mg/ml) incubations were carried out in 50 mM phosphate buffer, pH 7.4 in the presence of desired Gdn-HCl concentration for 4 h at 25 °C

0.75 M Gdn-HCl is indicative of perturbance in the micro-environment of trp. Consistent decrease in class S and increase in class II from 1.0 to 3 M Gdn-HCl indicated slight unfolding of the protein. In presence of 4 M Gdn-HCl, the spectrum of HRI (KD) was resolved into 12.7% class I trp in the hydrophobic environment and 87.3% class III which could be due to partial unfolding, while in presence of 5 and 6 M Gdn-HCl only class III was detected indicating fully exposed trp residues to the solvent.

Figure 1d represents Gdn-HCl induced changes in parameter A value ($A = I_{320}/I_{365}$, which is characteristic of the shape and position of the fluorescence spectrum [25, 26]) that decreases in presence of 0.25 M Gdn-HCl and remains constant up to 0.5 M indicating the presence of a stable intermediate. The parameter increases slightly at 0.75 M Gdn-HCl, and then gradually decreases with further increase in the denaturant concentration indicating multi-step unfolding of the protein.

Renaturation (10 times dilution of each sample) facilitates refolding of the protein completely up to 0.75 M Gdn-HCl, partially up to 4 M and to a substantial extent for 5–6 M Gdn-HCl denatured samples. This is indicated by recovery of parameter A (Fig. 1d). Thus, the totally unfolded protein regains the partially folded structure after renaturation. While refolding there is a stable intermediate formation of native-like intermediates between 1.0–1.5 M denaturant concentrations.

The phase diagram, which is considered as a sensitive tool to characterize the folding intermediate(s) [27, 28], was constructed by monitoring the change of the intensity at 365 nm as a function of the same at 320 nm (Fig. 2). Generally a straight line plot in the diagram reflects "all or none" process, while the non-linear relation between I_{320} and I_{365} indicates structural transitions involving folding intermediate(s). For the latter case, the intersection of the two lines indicates the appearance of an intermediate at the corresponding Gdn-HCl concentration. The phase diagram in the present study shows three linear portions in the data analysis for the unfolding transition, two of them intersecting at 0.75 M and others at 1.5 M Gdn-HCl, indicating the presence of stable intermediates at these concentrations. The phase diagram was insensitive to the intermediate state at 0.25 M Gdn-HCl (with only 20% fluorescence intensity compared to native HRI (KD)), whereas a third intermediate state appeared at 1.5 M. The intersection of the two lines observed for refolding transition also indicated the same. Therefore the overall process of Gdn-HCl mediated unfolding of HRI (KD) (i.e. transition from native, N, to the unfolded state, U) is characterized by the formation of at least three intermediate conformations, Int_1, Int_2 and Int_3, which are populated at around 0.25, 0.75 and 1.5 M Gdn-HCl, respectively. Further analysis of Int1 and Int2 by hydrophobic dye (ANS) binding indicated altered exposure of hydrophobic patches on the surface of the protein as the extent of dye binding was less for these samples as compared to the native protein (data not shown).

The CD studies indicated that there is a major retention of the secondary structure in HRI (KD) treated with 0.25–1.5 M Gdn-HCl. Figure 3 represents Gdn-HCl induced changes in MRE values recorded at 217 nm. The figure shows that between 0 and 1.5 M Gdn-HCl, the MRE_{217} values almost remain constant, suggesting the formation of native like intermediates with respect to the secondary structure.

Thus, Int_1 and Int_2 possess native-like secondary structure with 80% and 20% reduction in the fluorescence emission, respectively, which could be due to the changes

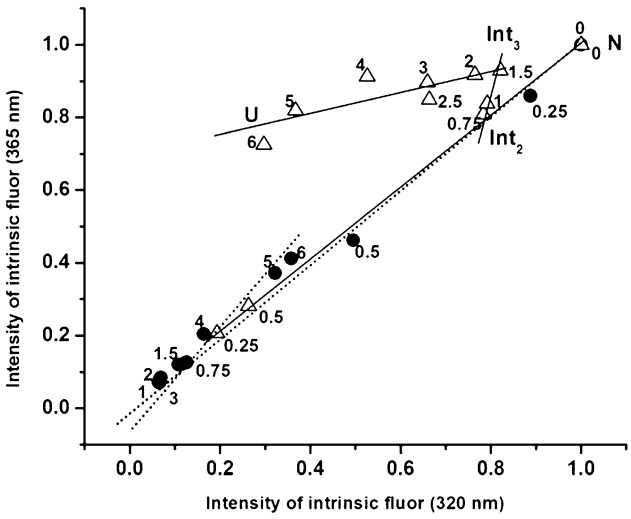

Fig. 2 Phase diagram representing the unfolding (*empty triangles*) and refolding (*filled circles*) of HRI (KD) induced by increasing Gdn-HCl concentration. Gdn-HCl concentration values are indicated in the vicinity of the corresponding symbol

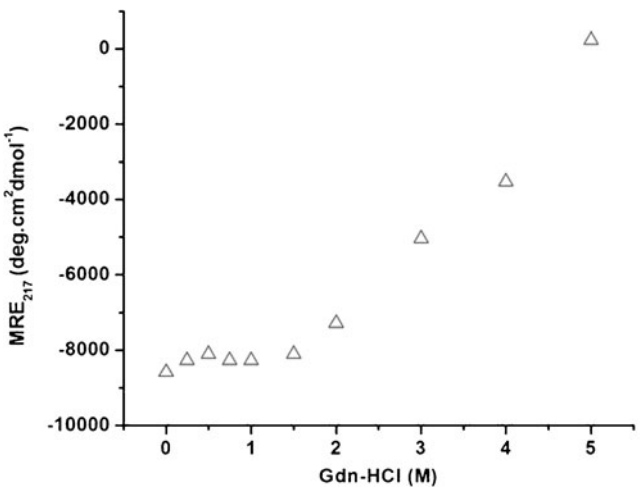

Fig. 3 Plot of CD (MRE_{217}) values of HRI (KD) (0.1 mg/ml) versus Gdn-HCl concentration

in microenvironment of trp. Int_3 showed slightly unfolded structure (3 nm red shift of λ_{max}) (inset Fig. 1a).

Effect of pH

Fluorescence Studies

The fluorescence emission spectra of HRI (KD) showed maximum fluorescence intensities in the pH range 7.0–9.0 and low intensity at extreme acidic and alkaline pH due to quenching of the intrinsic fluorescence because of protonation and deprotonation of the surface amino acids (data not shown).

Far UV and Near UV CD Spectra

Far UV CD spectra of the protein samples incubated at pH 3.0, 7.4 and 12.0 are shown in Fig. 4a. The CD spectra of native protein showed double minima at 208 and 217 nm. The calculation of secondary structure elements was carried out using CDPro (Continll) program available online (http://lamar.colostate.edu/~sreeram/CDPro/main.html). The calculated α-helical and β-sheet contents of HRI (KD) under different conditions are listed in Table 1. The values of the secondary structure elements were taken from Continll which gave the least NRMSD value. The analysis showed that the native protein contained 11.8% α-helix, 31.7% β-sheet, 23.5% β-turns and 33% unordered structures, indicating predominance of β-sheet structure. At pH 3.0, increase in negative ellipticity indicating a compact structure with major retention of secondary structure elements was observed (Table 1). The negative ellipticity at 217 nm reduced substantially at extreme alkaline pH indicating loss in the β-sheet content (Fig. 4a).

Near UV CD spectrum of native, and HRI (KD) incubated at pH 3.0 are shown in Fig. 4b. The changes in CD spectra of the protein from 250 to 300 nm were recorded for both these samples and compared. The positive ellipticity peaks at 263, 271 and 284 nm and a single negative ellipticity peak at 279 nm were observed for native HRI (KD). The ordered tertiary structure of HRI (KD) is significantly altered at pH 3.0. The minimum observed at 279 nm is completely lost in pH 3.0 incubated sample indicating major change in the tyrosine environment. Both far and near UV CD spectra of HRI (KD) at pH 3.0 showing a compact secondary structure and altered tertiary structure, respectively, are indicative of an acid-induced molten globule state for the protein. To further confirm this, hydrophobic dye binding of HRI (KD) was carried out under these conditions.

ANS Fluorescence

ANS has been shown to bind to hydrophobic regions of partially unfolded proteins that become exposed to the solvent [29]. The treatment of HRI (KD) with ANS showed negligible fluorescence at pH 7.4 and 12.0. The emission

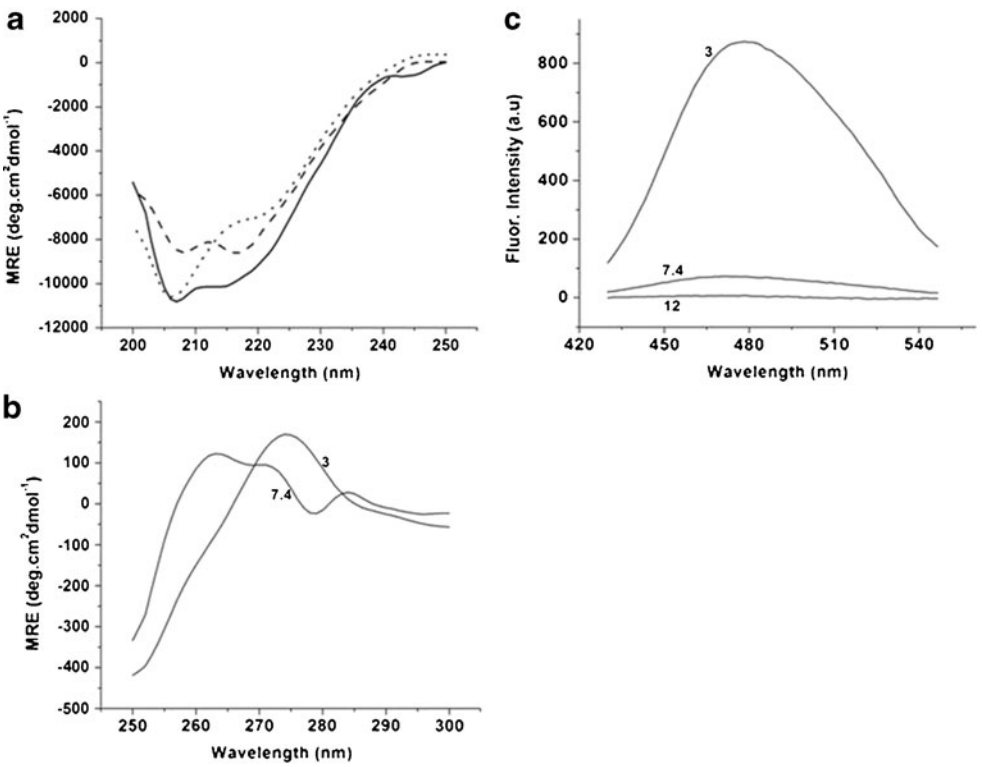

Fig. 4 pH induced conformational changes in HRI (KD). **a** Far UV CD spectra of native HRI (KD) (0.1 mg/ml) (– – –), acid induced state at pH 3.0 (——) and pH 12.0 induced state (····). **b** near-UV (1 mg/ml) CD spectra of HRI (KD) incubated at different pH. **c** ANS fluorescence emission spectra of HRI (KD) (5–10 μg/ml) at different pH. The samples were excited at 375 nm. The numbers on the spectra indicate the respective pH value. All pH incubations were carried out for 4 h in the respective buffers at 25 °C

Table 1 Secondary structure elements of HRI. The far-UV CD spectra of the HRI under different conditions were analyzed by Continll (CDPro) programme available online and data presented in percentage value. (The reference set used is SMP56, I Basis-10)

Environment	Helix	Sheet	Turns	Other	NRMSD[a]
Native	11.8	31.7	23.5	33.0	0.01
pH 3.0	19.1	26.4	21.4	33.0	0.02
Gdn-HCl (3 M)	3.3	52.9	23.3	19.5	0.07
Temp 95 °C (pH 3.0 sample)	10.1	29.4	22.8	37.7	0.10

[a] The agreement between experimental and calculated spectra was high with an NRMSD value less than 0.1

intensity seen for pH 3.0 incubated sample was enormous (almost ten times in comparison to pH 7.4 incubated sample) with simultaneous blue shift of the λ_{max} to ~480 nm (Fig. 4c). This suggests that at pH 3.0, hydrophobic amino acids are exposed to the surface causing enhanced binding of the dye. The readjustment of acidic pH to native pH showed no ANS binding (data not shown). Thus data presented in Fig. 4 showed that HRI (KD) retains significant secondary structure even at extreme acidic pH and confirmed the presence of a reversible acid-induced molten globule structure.

Characterization of Molten Globule

The molten globule-like structure observed at pH 3.0 was further characterized by thermal and chemical denaturation. The magnitude of negative ellipticity (MRE_{208}) decreases with temperature rise for both native and pH 3.0 incubated HRI (KD) (Fig. 5a). The T_m of the protein calculated for pH 3.0 and pH 7.4 incubated samples were 68.8 °C and 58.5 °C, respectively. There is also ~53% retention of the α-helical content in the pH 3.0 incubated protein at 95 °C when compared with unheated sample at the same pH indicating increased stability of the molten globule state (Table 1). Even at temperatures above 70 °C there is considerable retention of the α-helical content (indicated by MRE_{208} values) for the native protein signifying the thermo-stable nature of HRI (KD) (Fig. 5a).

The results of Gdn-HCl mediated denaturation of HRI (KD) at pH 3.0 were compared with the protein under similar conditions at pH 7.4 (Fig. 5b). Retention of the secondary structure was more at pH 3.0 than at pH 7.4 in the denaturation condition used, which confirmed the rigidness of the pH 3.0 intermediate structure of HRI (KD). Thus, increased T_m and more retention of the secondary structure elements in presence of 2 M Gdn-HCl indicates higher stability or rigidness of the molten globule-like intermediate existing at pH 3.0.

Fluorescence Life Time Measurement and Quenching Studies

Life Time Measurement

The fluorescence decay of the native HRI (KD) on a nanosecond (ns) time scale obtained from time resolved measurements is presented in Fig. 6. Tri-exponential curve could be fitted to time resolved fluorescence profile of HRI (KD) (χ^2=1.02). From this fit, three decay times τ_1 (0.38 ns), τ_2 (1.69 ns) and τ_3 (4.87 ns) were estimated with their relative contributions to the overall fluorescence being 34%, 38% and 28%, respectively, indicating the presence of three populations of trp conformers present in HRI (KD) (Table 2). The shorter lifetime component is supposed to be on the surface of the protein and its fluorescence decays faster while longer lifetime component

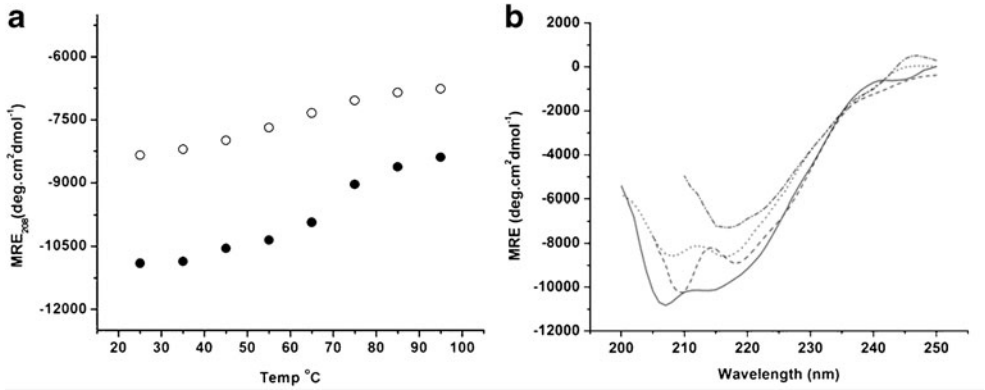

Fig. 5 Characterization of acid-induced molten globule state of HRI (KD). **a** Plot of MRE_{208} values of native HRI (KD) (*empty circle*) and pH 3.0 incubated HRI (KD) (*filled circle*) as a function of different temperatures starting from 25 °C to 95 °C with an interval of 10 °C. The protein was incubated for 10 min at different temperatures. **b** Far UV CD spectra of native HRI (KD) (0.1 mg/ml) (· · · ·), acid induced state at pH 3.0 (——), HRI (KD) incubated in 2 M Gdn-HCl at pH 7.4 (— · — ·), HRI (KD) incubated in 2 M Gdn-HCl at pH 3.0 (– – –). All protein incubations were carried out for 4 h in appropriate buffers

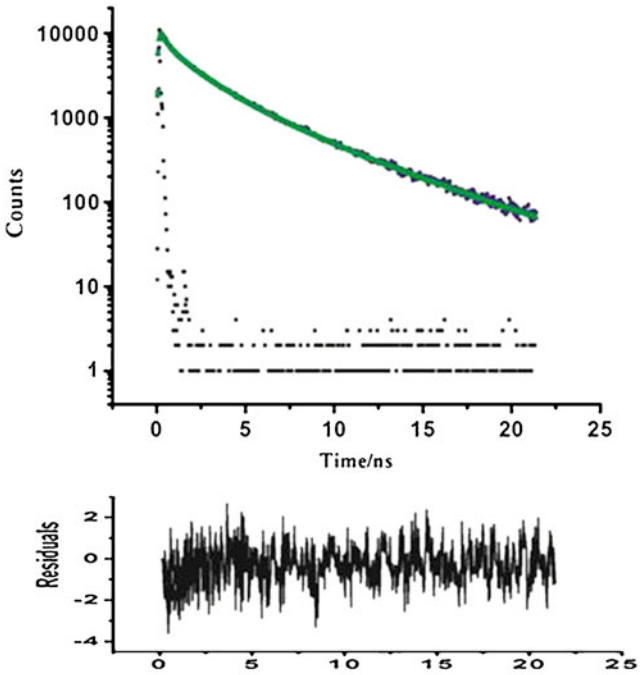

Fig. 6 Life time measurement of HRI (KD). Time resolved fluorescence decay profile of native HRI (KD). The solid line corresponds to the nonlinear least square fit of the exponential data. The lower panel represents the residual

is in the interior of the protein and decays slowly. The component with the intermediate value of life time (τ_2= 1.69 ns) could be due to the conformer present partly in hydrophobic and remaining in the hydrophilic environment. The three lifetimes of the protein can be correlated with the steady-state profile of HRI (KD) showing polar as well as nonpolar environment of trp. The average lifetime was calculated using the following equation [30]:

$$\tau = \sum_i \alpha_i t_i / \sum_i \alpha_i \quad i = 1, 2 \ldots . \tag{1}$$

where, τ is the average lifetime and α is the weighting factor. The average lifetime τ obtained is 2.13 ns for native HRI (KD) (Table 2). The average lifetime for 6 M Gdn-HCl denatured protein reduced to 1.98 ns and 0.85 ns in absence of any quencher and in presence of 0.4 M acrylamide, respectively. The value of the average lifetime of the native protein τ is not altered significantly after denaturation. However, the 3 individual components, τ_1, τ_2, τ_3 have changed significantly. The shortest lifetime component is converted to the longest; the longest to the medium and the medium lifetime component is converted to the shortest.

Fluorescence Quenching Studies

Analysis of the Steady-State Quenching Data The exposure and environment of the trps in HRI (KD) was investigated

Table 2 Parameters obtained from lifetime measurement of HRI under various conditions

Samples	Fluorescence life times, ns	Relative%	Average lifetime τ (ns)	Chi.sq $(\chi)^2$
Native (Nat)	0.38 (τ_1)	34	2.13	1.02
	1.69 (τ_2)	38		
	4.87 (τ_3)	28		
Denat (6 M Gdn-HCl)	3.99 (τ_1)	44	1.98	1.09
	0.69 (τ_2)	12		
	2.02 (τ_3)	44		
Denat + 0.4 M acrylamide	0.62 (τ_1)	58	0.85	1.09
	5.20 (τ_2)	07		
	1.60 (τ_3)	35		

by solute quenching technique using steady-state and time-resolved fluorescence studies. Quenching data obtained for all the quenchers used in this study were analyzed by the Stern-Volmer and modified Stern-Volmer equations as described previously [19, 30]. The fluorescence parameters obtained are presented in Table 3.

Quenching with Acrylamide Quenching of the intrinsic fluorescence of HRI (KD) gave a linear Stern-Volmer plot under native condition and showed a positive curvature for denatured protein (Fig. 7a and c). The K_{sv} value for native protein was 4.89 M^{-1}. Bimolecular quenching constant observed for acrylamide quenching was 2.3×10^9 $M^{-1}s^{-1}$ for native protein. Among the three quenchers used, acrylamide was the most efficient one as it could penetrate into the interior of the protein. As seen in Table 3, 74% of the total fluorescence of the native protein was accessible to acrylamide under native condition and 100% accessibility was observed upon denaturation due to unfolding as determined from the modified Stern-Volmer plot (Fig. 7b and d).

Quenching with Iodide and Cesium Ions The Stern-Volmer plot obtained for I^- quenching under native condition showed a downward curve indicating the presence of two populations of trp, one getting quenched faster (K_{sv1}= 1.91 M^{-1}) than the other (K_{sv2}=1.02 M^{-1}) (Fig. 7a). For Cs^+ quenching, the value of K_{sv} is 0.79 M^{-1}. The higher extent of quenching by I^- indicates slightly higher density of positive charge around the surface trp conformer. The denatured protein gave a linear Stern-Volmer plot (Fig. 7c) and the K_{sv} values obtained were 1.33 M^{-1} and 5.58 M^{-1} for Cs^+ and I^-, respectively, indicating change in the conformation of the protein. From Table 3 it is seen that the total fluorescence of the native protein accessible to Cs^+ and I^- ions increased upon denaturation due to conforma-

Table 3 Summary of parameters obtained from Stern-Volmer and modified Stern-Volmer analysis of the intrinsic fluorescence quenching of HRI with different quenchers

Quencher and state	K_{sv1} (M^{-1})	K_s (M^{-1})	k_{q1}($\times 10^9$ $M^{-1}s^{-1}$)	K_{sv2} (M^{-1})	k_{q2}($\times 10^9$ $M^{-1}s^{-1}$)	*f*a	*K*a (M^{-1})
Acrylamide							
Native	4.89	–	2.3	–	–	0.74	8.5
Denatured	3.08	5.62	1.56	–	–	1	4.33
KI							
Native	1.91	–	0.9	1.02	0.48	0.41	8.3
Denatured	5.58	–	4.39	–	–	0.74	11.33
CsCl							
Native	0.79	–	0.38	–	–	0.17	11.54
Denatured	1.33	–	1.05	–	–	0.72	2.23

tional changes. Low bimolecular quenching constants indicated low collision frequency.

Determination of Collisional and Static Quenching Constants The profile obtained for acrylamide quenching of denatured HRI (KD) showed a positive curvature suggesting involvement of both collisional and static components in quenching (Fig. 7c). Hence the data was analyzed using Eq. 2 which resolves the dynamic and static components [25].

$$F_0/F_c = (1 + K_{sv}[\mathrm{Q}])(1 + K_s[\mathrm{Q}]) \quad (2)$$

Where K_{sv} is the Stern-Volmer (dynamic) quenching constant, K_s is the static quenching constant and [Q] is the quencher concentration. The dynamic quenching constant reflects the degree to which the quencher achieves the encounter distance of the fluorophore and can be determined by the fluorescence lifetime measurements according to the Eq. 3 [31].

$$\tau_0/\tau = (1 + K_{sv}[\mathrm{Q}]) \quad (3)$$

Where τ_0 is the average lifetime in absence of the quencher and τ is the average lifetime in presence of a quencher at a concentration [Q]. Lifetime measurement

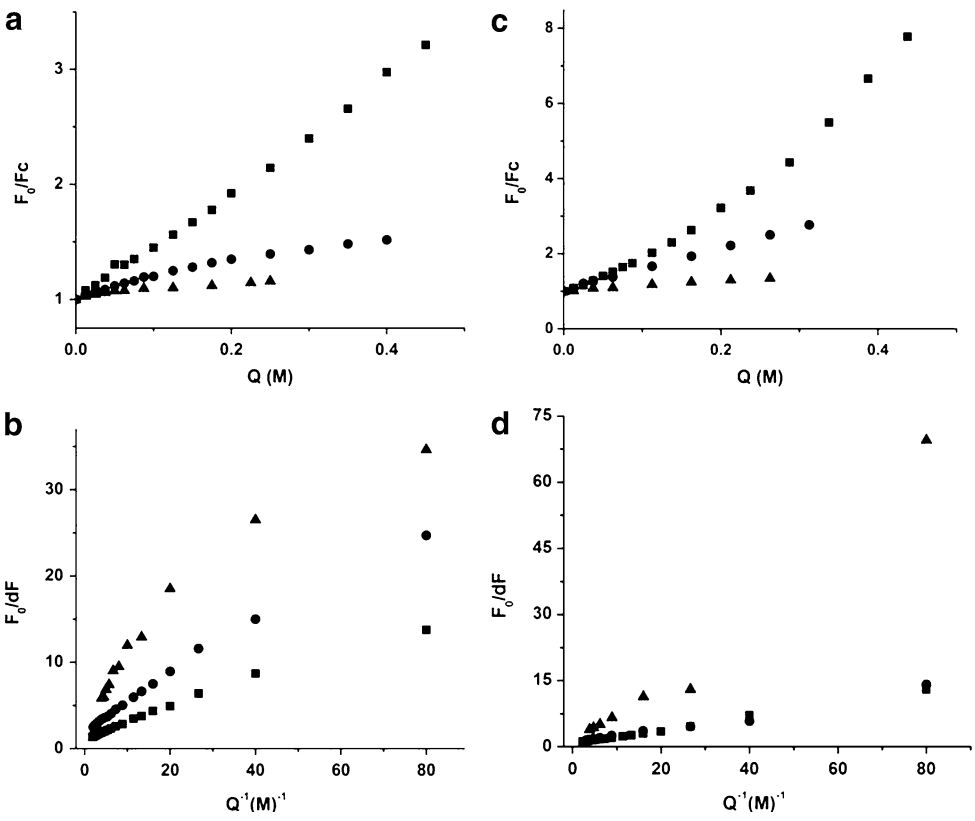

Fig. 7 Stern-Volmer plots (**a** and **c**) and modified Stern-Volmer plots (**b** and **d**) for the quenching of native (**a** and **b**) and 6 M Gdn-HCl denatured (**c** and **d**) HRI (KD) (0.03 mg/ml). Acrylamide (*filled square*), iodide (*filled circle*) and cesium (*filled triangle*) were used as the quenchers. After fitting the data the R value in each case was 0.99. The downward curve seen in the quenching profile of iodide under native condition (**a**) split into two linear components and the remaining data after fitting gave R=0.99

data of fluorescence emission of HRI (KD) obtained for acrylamide quenching was used in the Eq. 3 to obtain the K_{sv} value (Fig. 8a). The K_{sv} value obtained was 3.08 M^{-1}. Incorporating this value in Eq. 2 and plotting a graph of $(F_0/F_c)/(1+K_{sv}[Q])$ against [Q], the value of the static quenching constant (K_s) was obtained as 5.62 M^{-1} (Fig. 8b) and the bimolecular quenching constant, k_q was calculated as $k_q=K_{sv}/\tau$ and was found to be 1.56×10^9 $M^{-1}s^{-1}$. Incorporating the values of K_{sv} and K_s in the expression $(1+K_{sv}[Q])(1+K_s[Q])$, the values obtained were plotted against [Q]. It was observed that the values of F_0/F_c and $(1+K_{sv}[Q])(1+K_s[Q])$ match very well (Fig. 8c). The relative percentage of shorter lifetime component increased while that of longer lifetime component decreased with increasing quencher concentration. This suggests that more of trp populations get exposed on the surface due to unfolding of the protein but a residual structure is still retained within.

Conclusion

The heme-regulated eIF2α kinase (HRI) belongs to the class of stress response proteins. Our study was primarily aimed at understanding the conformational transitions and stability of HRI (KD) under different denaturing conditions. In summary, our data on the fluorescence and CD spectroscopic analysis of HRI (KD) unfolding illustrate the diversity of unfolding pathways for the given protein. The unfolding (Gdn-HCl mediated) mechanism of HRI (KD) is a multi-state process involving three intermediates with different properties. CD analysis of the native protein depicts the presence of more of β-sheets and lesser α-helices. pH and thermal denaturation studies along with ANS binding confirmed the presence of an acid-induced molten globule structure, which is a very compact and rigid form of HRI (KD). The analysis of the fluorescence spectra of the native protein revealed the presence of trp populations in HRI (KD) in hydrophobic as well as bonded to structured water. Upward curvature of Stern-Volmer plot, three lifetimes (Table 2), and 60% reduction in the average lifetime of acrylamide quenched denatured HRI (KD) indicated static as well as dynamic quenching of trp fluorescence due to change in the conformation of the protein. Surface trp(s) seem(s) to have two populations or conformers, τ_1 and τ_2, both contributing substantially to the total fluorescence.

Multistate unfolding of the protein in the vicinity of Gdn-HCl could be because of the differential unfolding of the three domains, Kinase 1, Kinase Insertion, and Kinase 2 [1, 32]. The protein is also able to attain a compact and rigid molten globule like structure at extreme acidic pH. Our results indicate the inherent structural stability of HRI (KD), a member of the class of stress response proteins.

HRI is in focus as a key regulatory molecule of translational regulation. There are no available crystal structures or other data on the structural transitions of HRI (KD) under various denaturing conditions till date. Hence the results of our study focus on these aspects and provide important information with respect to the folding/unfolding pathways leading to HRI (KD) intermediate structural forms during the folding/unfolding process. Understanding of molten globule or partially unfolded states is also very important because they are the starting point of the process by which folding to the active form of protein is achieved following the biosynthesis in most cases. Further structural characterization of these intermediate forms of the protein can be undertaken to have a better picture of the tertiary conformational topology in HRI.

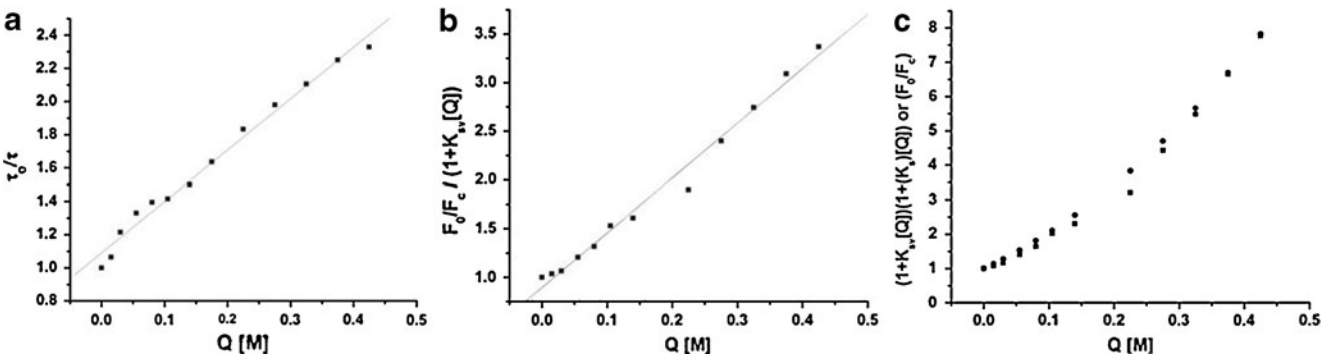

Fig. 8 Quenching of denatured HRI (KD) fluorescence with acrylamide on time resolved spectrofluorimeter. **a** The plot of τ_0/τ for the quenching data of HRI (KD) with acrylamide in denatured condition. **b** The plot of $(F_0/F_c)/(1+K_{sv}[Q])$ against [Q]. **c** The plot of F_0/F_c (■) or $(1+K_{sv}[Q])(1+K_s[Q])$ (●) against [Q]

Acknowledgments Financial assistance from DST, Govt. of India [Grant number SR/SO/BB-72] and DAE/BRNS [Grant number 2007/37166/BRNS] to JKP is duly acknowledged. The authors wish to thank Dr. Arvind Sahu, NCCS, Pune, and Prof. G. Krishnamoorthy, TIFR, Mumbai for permitting to use the CD spectrometer and time-resolved fluorescence facility, respectively. SRK and VB thank DBT, Govt. of India, and AK thanks UGC, Govt. of India for a research fellowship.

References

1. Chen J-J, London IM (1995) Regulation of protein synthesis by heme-regulated eIF-2α kinase. Trends Biochem Sci 20:105–108
2. Chen J-J (2000) In: Sonenberg N, Hershey JWB, Mathews MB (eds) Translational control of gene expression. Cold Spring Harbor Laboratory Press, New York, pp 529–546
3. Dever TE (2002) Gene-specific regulation by general translation factors. Cell 108:545–556
4. Chen J-J, Throop MS et al (1991) Cloning of the cDNA of the heme-regulated eukaryotic initiation factor 2α (eIF-2α) kinase of rabbit reticulocytes: homology to yeast GCN2 protein kinase and human double stranded-RNA-dependent eIF-2α kinase. Proc Natl Acad Sci USA 88:7729–7733
5. Meurs E, Chong K et al (1990) Molecular cloning and characterization of human double-stranded RNA activated protein kinase induced by interferon. Cell 62:379–390
6. Harding HP, Zhang Y, Ron D (1999) Protein translation and folding are coupled by an endoplasmic-reticulum-resident kinase. Nature 397:271–274
7. Chong KL, Feng L et al (1992) Human p68 kinase exhibits growth suppression in yeast and homology to the translational regulator GCN2. EMBO J 11:1553–1562
8. Liu S, Bhattacharya S et al (2008) Haem-regulated eIF2alpha kinase is necessary for adaptive gene expression in erythroid precursors under the stress of iron deficiency. Br J Haematol 143:129–137
9. Pal JK, Chen J-J, London IM (1991) Tissue distribution and immunoreactivity of heme-regulated eIF-2α kinase determined by monoclonal antibodies. Biochemistry 30:2555–2562
10. Han AP, Yu C et al (2001) Heme-regulated eIF2alpha kinase is required for translational regulation and survival of erythroid precursors in iron deficiency. EMBO J 20:6909–6918
11. Rafie-Kolpin M, Chefalo PJ et al (2000) Two heme-binding domains of heme-regulated eukaryotic initiation factor-2alpha kinase. N terminus and kinase insertion. J Biol Chem 275:5171–5178
12. Petrov T, Rafols JA et al (2003) Cellular compartmentalization of phosphorylated eIF2α and neuronal NOS in human temporal lobe epilepsy with hippocampal sclerosis. J Neurol Sci 209:31–39
13. Mellor H, Flowers KM et al (1994) Cloning and characterization of cDNA encoding rat hemin-sensitive initiation factor-2α (eIF-2α) kinase. Evidence for multitissue expression. J Biol Chem 269:10201–10204
14. Berlanga JJ, Herrero S, Haro C (1998) Characterization of the hemin-sensitive eukaryotic initiation factor 2α kinase from mouse nonerythroid cells. J Biol Chem 273:32340–32346
15. Lu L, Han AP, Chen J-J (2001) Translation initiation control by heme-regulated eukaryotic initiation factor 2α kinase in erythroid cells under cytoplasmic stresses. Mol Cell Biol 21:7971–7980
16. Matts RL, Schatz JR et al (1991) Toxic heavy metal ions activate the heme-regulated eukaryotic initiation factor-2α kinase by inhibiting the capacity of hemin supplemented reticulocyte lysates to reduce disulfide bonds. J Biol Chem 266:12695–12702
17. Pal JK, Anand S, Joseph J (1996) Association of HSP90 with the heme-regulated eukaryotic initiation factor 2α kinase-A molecular collaboration for regulating protein synthesis. J Biosci 21:191–205
18. Chen J-J, Yang JM et al (1989) Disulfide bond formation in the regulation of eIF-2α kinase by heme. J Biol Chem 264:9559–9564
19. Sreejith RK, Yadav VN et al (2009) Conformational characterization of human eukaryotic initiation factor 2α: A single tryptophan protein. Biochem Biophys Res Commun 390:273–279
20. Singh AK, Mullick J et al (2006) Functional characterisation of the complement control protein homolog of herpes virus saimiri: ARG-118 is critical for factor I cofactor activities. J Biol Chem 281:23119–23128
21. White J, Lukacik P et al (2004) Biological activity, membrane-targeting modification, and crystallization of soluble human decay accelerating factor expressed in *E. coli*. Protein Sci 13:2406–2415
22. Laemmli UK (1970) Cleavage of structural proteins during the assembly of the head of bacteriophage T4. Nature 227:680–685
23. Towbin H, Staehelin T, Gordon J (1979) Electrophoretic transfer of proteins from polyacrylamide gels to nitrocellulose sheets: procedure and some applications. Proc Natl Acad Sci USA 76:4350–4354
24. Shen C, Menon R et al (2008) The protein fluorescence and structural toolkit: Database and programs for the analysis of protein fluorescence and structural data. Proteins 71:1744–1754
25. Turoverov KK, Haitlina SY, Pinaev GP (1976) Ultra-violet fluorescence of actin. Determination of actin content in actin preparations. FEBS Lett 62:4–6
26. He H-W, Zhang J et al (2005) Conformational change in the C-terminal domain is responsible for the initiation of creatine kinase thermal aggregation. Biophys J 89:2650–2658
27. Su J-T, Kim S-H, Yan Y-B (2007) Dissecting the pretransitional conformational changes in aminoacylase I thermal denaturation. Biophys J 92:578–587
28. Bushmarina NA, Kuznetsova IM et al (2001) Partially folded conformations in the folding pathway of bovine carbonic anhydrase II: a fluorescence spectroscopic analysis. Chembiochem 2:813–821
29. Semisotnov GV, Radionova NA et al (1991) Study of the "molten globule" intermediate state in protein folding by a hydrophobic fluorescent probe. Biopolymers 31:119–128
30. Lakowicz EM, Weber G (1973) Quenching of protein fluorescence by oxygen: detection of structural fluctuations in proteins on the nanosecond time scale. Biochemistry 12:4171–4179
31. Lakowicz JR (1983) Principles of fluorescence spectroscopy. Plenum Press, New York
32. Chen J-J (2007) Regulation of protein synthesis by the heme-regulated eIF2α kinase: relevance to anemias. Blood 109:2693–2699